PREBIOTIC CHEMISTRY

Enhanced Photocatalytic Performance of ZnS for Reversible Amination of α-oxo Acids by Hydrothermal Treatment

Wei Wang · Qiliang Li · Xiaoyang Liu · Yanqiang Yang · Wenhui Su

Abstract To understand how life could have originated on early Earth, it is essential to know what biomolecules and metabolic pathways are shared by extant organisms and what organic compounds and their chemical reaction channels were likely to have been primordially available during the initial phase of the formation of prebiotic metabolism. In a previous study, we demonstrated for the first time the reversible amination of α-oxo acids on the surface of photo-illuminated ZnS. The sulfide mineral is a typical component at the periphery of submarine hydrothermal vents which has been frequently argued as a very attractive venue for the origin of life. In this work, in order to simulate more closely the precipitation environments of ZnS in the vent systems, we treated newly-precipitated ZnS with hydrothermal conditions and found that its photocatalytic power was significantly enhanced because the relative crystallinity of the treated sample was markedly increased with increasing temperature. Since the reported experimental conditions are believed to have been prevalent in shallow-water hydrothermal vents of early Earth and the reversible amination of α-oxo acids is a key metabolic pathway in all extant life forms, the results of this work provide a prototypical model of the prebiotic amino acid redox metabolism. The amino acid dehydrogenase-like chemistry on photo-irradiated ZnS surfaces may advance our understanding of the establishment of archaic non-enzymatic metabolic systems.

Keywords Prebiotic metabolism · Redox homeostasis · Photocatalysis · ZnS · Reversible amination

W. Wang (✉) · Y. Yang · W. Su
CCMST, Academy of Fundamental and Interdisciplinary Sciences, Harbin Institute of Technology, Harbin 150080, China
e-mail: wwang_ol@hit.edu.cn

Q. Li · X. Liu
State Key Lab of Inorganic Synthesis and Preparative Chemistry, College of Chemistry, Jilin University, Changchun 130012, China

Introduction

Scenarios for how life originated on early Earth have received much attention in the literature of prebiotic evolution. Since metabolism is of key importance for the functional expression of genetic polymers and the survival of terrestrial life, a primary question in those well-meant blueprints is how prebiotic metabolic systems could have evolved before the emergence of the last universal common ancestor. In living organisms, metabolic reactions are catalyzed by enzymes. However, an enzyme molecule only speeds up an existing reaction, but does not create new reactions. How prebiotic metabolic pathways (especially the abiotic synthesis of enzymes and their precursors) could have functioned before the emergence of the ancient enzymatic network is a critically important unanswered question. Perhaps the enzyme-assisted biochemical pathways in extant organisms are vestiges of early nonenzymatic metabolism.

This hypothesis is accepted today by many origin-of-life researchers. It has been frequently argued that life started with an infrastructure of specific physical and chemical processes (Wächtershäuser 1988; Fry 2011). According to this intriguing scenario, the emergence of the primordial metabolic systems may be postulated as a continuum from Earth's geochemical processes to life's biochemical procedures (Hartman 1975; Morowitz and Smith 2007; Cairns-Smith 2008). Sulfide mineral surfaces in hydrothermal vent systems have been often suggested as likely sites for such transformations (Wächtershäuser 1988; Russell and Hall 1997). The minerals may act as catalyst, a scaffolding, and a template for the prebiotic synthesis and directional assemblage of biomolecules (Orgel 1998) by using inherent chemical energy or extraneous thermal and light energy (Hazen 2001; Russell and Martin 2004; Boiteau and Pascal 2011; Simoncini et al. 2011). Based on these postulations, some surface reactions in aqueous metal sulfide systems have been developed to mimic common biochemical steps, and many interesting results have been achieved (Zhang and Martin 2006; Wächtershäuser 2007; Wang et al. 2011).

In a previous study, we reported a promising means of the rocky start of prebiotic amino acid metabolism, i.e., the reversible amination of α-oxo acids on photo-illuminated ZnS surfaces (Wang et al. 2012). ZnS is a prevalent constitute at the periphery of hydrothermal deposits (Edmond et al. 1995; Mulkidjanian 2009). As a common semiconductor, it can absorb solar light to generate photoelectrons and holes. The photogenerated charges may catalyze redox reactions for the primordial synthesis and chain extension of biomolecules such as α-oxo acids (Eggins et al. 1993; Guzman and Martin 2009) by using inorganic species as initial materials. Starting with α-oxo acids and ammonia, the photoelectrons ignite the reductive amination reaction to produce amino acids. In reverse, the amino acid products can be oxidized by the holes back to the oxo acids. The whole reversible process not only provides a new pathway for the abiotic synthesis of amino acids, but also suggests a non-enzymatic model for the prebiotic redox homeostasis between amino acids and oxo acids.

At the periphery of hydrothermal fields, the vent fluids is always overheated to 200–300°C. In the present study, to simulate the authentic precipitation environments of ZnS in the vent systems as closely as are presently known, newly-prepared ZnS colloids were treated under various hydrothermal conditions. The structure characteristics and photocatalytic activity of the ZnS samples were investigated in detail. The aim of this work is to examine the influence of hydrothermal treatment on the photocatalytic efficiency of ZnS and then to discuss the possible role of minerals during the emergence of primitive metabolic pathways.

Materials and Methods

Materials

L-amino acids (>99 %, Solarbio) and α-oxo acids (>98 %, Sigma) were used without further purification. All other chemicals (Sinopharm, China) were obtained in analytical grade, with the exception of methanol and acetonitrile which were of chromatographic grade. Ultrapure water (Millipore) was deoxygenated with high purity argon gas (99.999 %) by bubbling it through 1 L water (1 L/min) for 1 h. The deaerated water was used throughout.

Preparation and Characterization of ZnS

ZnS was precipitated with stirring by dropwise adding 20 mL of 0.3 M Na_2S to 15 mL of 0.4 M $ZnSO_4$. The mixture was sealed in a Telfon-lined stainless steel autoclave (70 % filled). All the above procedures were performed anaerobically inside a vacuum glove box kept under an argon atmosphere. After maintained in an oven at different temperatures for a selected period of time, the ZnS precipitate was collected by filteration, washed five times with 30 mL deionized water, sucked as dry as possible and finally dried in a vacuum at 30°C for 24 h. The ZnS solid was ground to 120 mesh before characterization and use. The as-prepared samples with different treatment temperatures/times 30°C/6 h, 100°C/6 h, 200°C/6 h, 200°C/12 h, and 200°C/24 h were referred as ZnS-1, ZnS-2, ZnS-3, ZnS-4, and ZnS-5, respectively.

The phase structure of ZnS was measured by powder X-Ray diffraction (XRD) experiments on a Rigaku Ultrima IV diffractometer. Specific surface area (SSA) analysis was carried out on a Micromeritics ASAP 2420 surface area and porosity analyzer.

Photochemistry Experiments

All photochemical reactions were conducted under argon atmosphere by using a self-devised experimental system with a 500 W mercury-xenon lamp. The general methodology has already been reported elsewhere (Wang et al. 2012).

Product Analysis

After irradiation for a selected time period, 1 mL of sample solution was withdrawn from the reaction vessel and passed through a 0.22 μm microvoid filter film. For the reductive amination experiment, the filtered sample was adjusted to pH 11 and then bubbled with argon (50 mL/min) for 30 min to remove excessive ammonia. The remnant solution (ca. 0.8 mL) was brought back to 1 mL with water before analysis. Pre-column derivatization methods were employed to determine the yields of the products by using a Waters 600E HPLC system with a C18 column (Phenomenex, Luna, 5 μm, 250×4.6 mm). The column separation was performed at a constant temperature of 28°C.

For amino acid analysis, in a 1 mL vial, 300 μL of 0.5 M NaHCO3 (pH 9) and 50 μL of 5 % 2,4-dinitrofluorobenzene/ acetonitrile were successively added to 50 μL of a standard mixture of amino acids (1 mM) or a sample solution. After being mixed adequately, the specimen was heated in darkness at 60°C for 30 min. When the sample was cooled down to the room temperature, 400 μL of 0.1 M KH2PO4 buffer (pH 7) was added to terminate the derivatization reaction. The following gradient elution program was used for the separation of amino acid derivatives: 0 min, 82 % A, 18 % B; 2 min, 67 % A, 33 % B; 11.5 min, 58 % A, 42 % B; 14 min, 46 % A, 54 % B; 32 min, 40 % A, 60 % B; 40 min, 20 % A, 80 % B, where A was 14 mM

Na$_2$HPO$_4$ (pH 8.2) and B was acetonitrile/water (1:1). The flow rate was 1.0 mL/min. The eluent was monitored at 360 nm by a UV detector. The program returned to initial conditions and re-equilibrated for 5 min before the next sample injection.

Alpha-oxo acid concentrations were determined as follows: In a 1 mL vial, 100 μL of 0.2 M NaOH, 100 μL of 0.2 M phenylhydrazine hydrochloride, and 600 μL of 0.1 M K$_2$HPO$_4$ (pH 7) were successively added to 10 μL of a standard mixture of oxo acids (1 mM) or a sample solution. The specimen was mixed well by shaking and left to stand at room temperature for 20 min. Then the sample was immediately chromatographed through the column. A mobile phase consisted of 95 % phosphate buffer (13 mM KH$_2$PO$_4$, 1 mM K$_2$HPO$_4$, pH 6) and 5 % methanol was used. The elution behaviors were monitored at UV 325 nm with a flow rate of 1.5 mL/min.

Results

We first examined the reductive amination reaction of pyruvate. In a typical run, 2 mmol ZnS was dispersed in 50 mL of a solution containing 1 mmol pyruvate, 100 mmol NH$_4$Cl, and 10 mmol Na$_2$SO$_3$. The solution was adjusted to pH 10 by using NaOH. This pH value was selected since the submarine seepage water in the early hydrothermal vent systems was suggested to be ultramafic (Russell and Hall 1997; Martin et al. 2008) and also because basic conditions are more conducive to the reductive amination reaction (Huber and Wächtershäuser 2003). The pH did not change during the photo-irradiation process since it was highly buffered by an ammonium-ammonia equilibrium. Figure 1a shows the yields of alanine catalyzed by different ZnS catalysts. It can be found that the hydrothermal treatment significantly enhanced the photocatalytic efficiency of ZnS. In the studied range, the higher the treatment temperature, the stronger the catalytic activity of ZnS. The yield of alanine catalyzed by ZnS-3 was about 2.5 times that formed by ZnS-1. However, it slightly declined with increasing the treatment time. Additionally, no trace of alanine was formed in the absence of ZnS. With no NH$_4$Cl or α-KG or without exposure to irradiation, also no alanine was detected (data not shown). The complete set of control experiments imply that the reductive amination of pyruvate is driven by the ZnS-assisted photochemical reaction.

In the oxidative deamination reaction, 1 mmol alanine was dissolved in a 50 mL suspension of 2 mmol ZnS. The photochemical experiment was conducted at pH 10. As the reaction progressed, a pronounced pH drop of about 0.5–1 pH unit occurred, possibly due to the release of protons from alanine to the environment (see details in the following text). To circumvent the influence of pH shift on the catalytic performance, the solution was regulated to pH 10 every 30 min. As expected, a similar trend among the catalytic efficiencies of different ZnS samples was observed (Fig. 1b), as in the reductive amination experiments (Fig. 1a). The yield of pyruvate catalyzed by ZnS-3 was about two times higher than that by ZnS-1.

The mechanism of the reversible amination reaction can be explained by the photo-electrochemical properties of ZnS. As an n-type semiconductor, ZnS can absorb UV photons to create photoelectrons (e$^-$) in the conduction band (CB) and holes (h$^+$) in the valance band (VB) (Fig. 2). The fates of the excited charges tend to fall into two camps: migrate to the particle surface (pathway A) or recombine in the volume of the particle (pathway B). The migrated charges may also recombine at the particle surface (pathway C). However, if an organic or inorganic species is pre-adsorbed on the surface, the separated charges may transfer to the species and catalyze redox reactions.

Fig. 1 Yields of (**a**) alanine and (**b**) pyruvate vs the irradiation time in the reductive amination and oxidative deamination experiments, respectively. Experimental conditions: (**a**) 2 mmol ZnS was dispersed in 50 mL of a solution containing 1 mmol pyruvate, 100 mmol NH_4Cl, and 10 mmol Na_2SO_3; (**b**) 2 mmol ZnS and 1 mmol alanine in 50 mL water. All reactions were conducted at pH 10 and 30°C
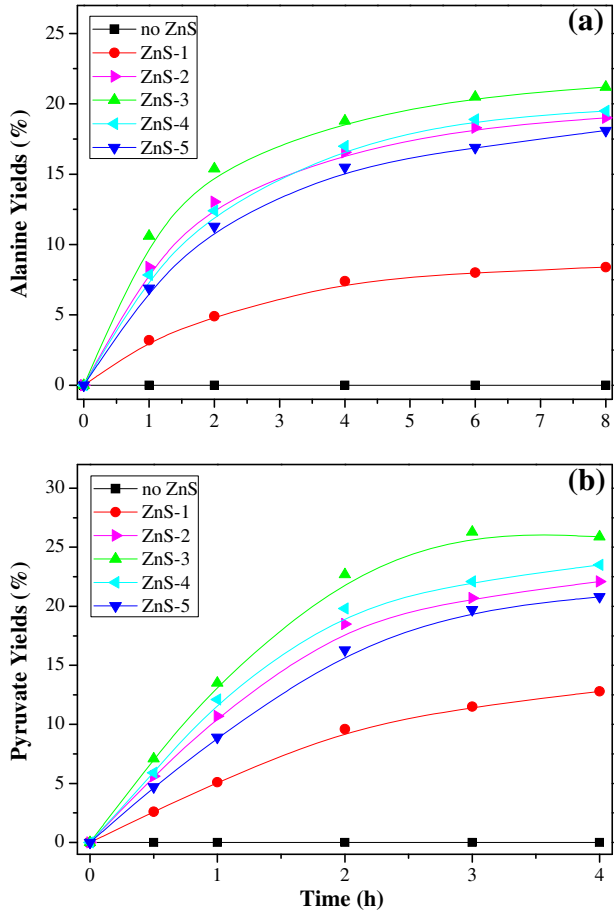
In water at pH 10, the energy levels of the conduction band and valence band of ZnS are located at −1.63 V and +1.97 V vs. NHE (normal hydrogen electrode), respectively. These properties make the photo-illuminated ZnS surface a strong electrochemical anode and a
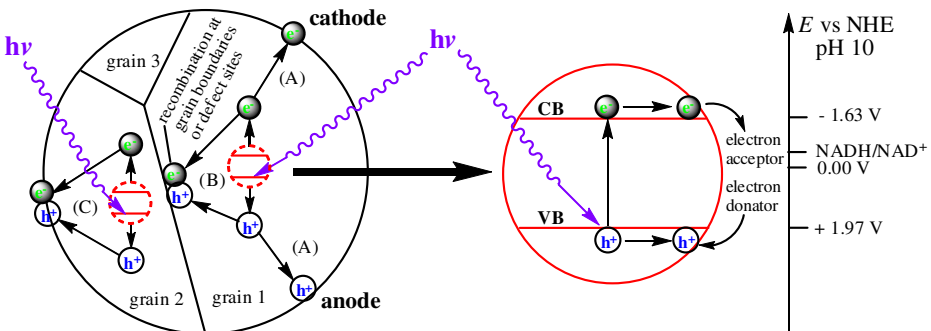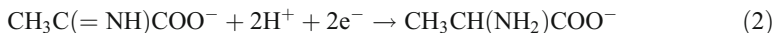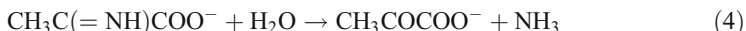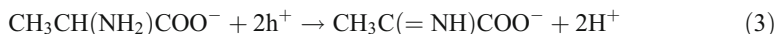

Fig. 2 Schematic diagram of the deexcitation events in a ZnS particle after photoexcitation. The energy levels were calculated for aqueous solution using standard electrode potentials (Xu and Schoonen 2000) with the Nernst equation at 25°C

cathode. The reductive amination of pyruvate occurs on the cathode through a Shiff base intermediate according to

$$CH_3COCOO^- + NH_3 \rightarrow CH_3C(= NH)COO^- + H_2O \tag{1}$$

$$CH_3C(= NH)COO^- + 2H^+ + 2e^- \rightarrow CH_3CH(NH_2)COO^- \tag{2}$$

In living organisms, reaction (2) is reversibly catalyzed by alanine dehydrogenase (Nitta et al. 1974), by using NADH as the electron donor ($E=-0.5$ V, pH 10). We have no information about the redox potential of Eq. 2. However, since the conduction band of ZnS is located at a much more negative potential than NADH/NAD$^+$ (Fig. 2), it facilitates the reductive amination of pyruvate by using the photogenerated electrons. Na$_2$SO$_3$ was added as a sacrificial agent which acted as an electron donor to fill the holes. It not only avoided the oxidation of organic compounds by the holes, but also reduced the recombination of the photoelectrons with the holes. Therefore it made more efficient the reductive amination of pyruvate. In the absence of Na$_2$SO$_3$, the photoreaction efficiency decreased by about 3 times; the yield of alanine after 8 h irradiation was only 7.2 % by using ZnS-3.

In reverse, alanine can be oxidized to pyruvate by the holes left behind in the valence band of ZnS (Wang et al. 2012). The electron-deficient hole has a high oxidative potential. It is apt to grab electron from the α-N or α-C atom of alanine, just like a hydroxyl radical (Bonifačić et al. 1998). Alanine undergoes two successive steps of one-electron oxidation to the Schiff base intermediate which subsequently is hydrolyzed to release pyruvate and ammonia (Ohtani et al. 1995).

$$CH_3CH(NH_2)COO^- + 2h^+ \rightarrow CH_3C(= NH)COO^- + 2H^+ \tag{3}$$

$$CH_3C(= NH)COO^- + H_2O \rightarrow CH_3COCOO^- + NH_3 \tag{4}$$

As far as is concerned the strengthening effect of hydrothermal treatment on the catalytic activity of ZnS, it can be explained by the phase structure changes of the semiconductor particle. Figure 3 shows the XRD patterns of the as-prepared ZnS samples. The set of wide angle XRD spectra illustrate that ZnS crystallizes as a single phase. All the peaks could be attributed to the cubic zinc blende structure of ZnS (JCPDS file No. 65–0309). At 30°C, the broadness of the major diffraction peaks indicates the formation of nanocrystals. Diffraction peaks from (200), (331), and (400) planes does not appear in XRD patterns of ZnS-1 and ZnS-2 since they have submerged in the background due to their small crystal size and large line broadening. After treatment at 100 and 200°C, the peaks become higher and sharper, indicating largely grown grains with higher crystallinity (Table 1). In a ZnS particle composed of many crystallites/grains, the larger the crystallite size the smaller the total surface area of grain boundaries. Meanwhile, the better the crystallinity the less the defect sites. Such improvements decrease the possibility of photoelectron–hole recombination in the volume of the particle (Fig. 2), thereby leading to higher catalytic activity. However, it is not true that the bigger the crystallites the better the catalytic power. When the grain size gets bigger, the distance that photogenerated charges have to migrate to surface reaction sites becomes longer and results in an increase in the recombination probability. This may help to explain the decrease of the catalytic efficiencies of ZnS-4 and ZnS-5 compared to that of ZnS-3.

The photoreactions depend on the direct contact of the organic compounds with the solid ZnS surfaces. Therefore, as well as the internal structural properties, the specific surface area

Fig. 3 XRD patterns of the pre-
pared ZnS samples
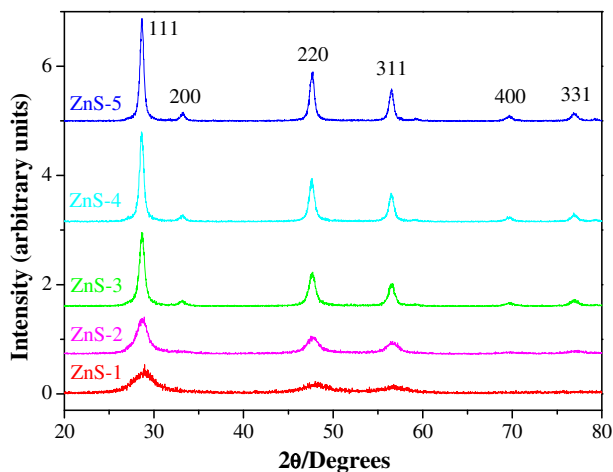
(SSA) of ZnS particles is also a key parameter determining the catalytic efficiency in the heterogeneous photochemical reactions. We analyzed the SSA of all ZnS samples. However, the results show no fold difference among the specific area data of different ZnS samples which vary from 106.8 m^2/g to 167.2 m^2/g (Table 1). Especially, the most active catalyst ZnS-3 does not have the largest specific area. Thus in the present study the alterations of the photocatalytic efficiencies of different ZnS samples involve their internal structural changes but are independent of the SSA.

To identify with more certainty the reaction mechanisms stated above, we extended the ZnS-photo-promoted reaction model to the reductive amination of α-ketoglutarate and α-ketoisovalerate and the oxidative deamination of their corresponding amino acids, i.e., glutamate and valine. The results are represented in Fig. 4. Both the reversible amination reaction pathway and the enhancing effect of hydrothermal treatment on the photocatalytic activity of ZnS were further confirmed.

Discussion

Since the discovery of the first submarine hydrothermal vent in 1977 (Corliss et al. 1979), it has been frequently argued as a congenial site for the origin of terrestrial life (Baross and Hoffman 1985; Wächtershäuser 1988; Holm 1992; Russell and Hall 1997; Martin et al. 2008). The hydrothermal chimneys are composed of various metal sulfide minerals. Among these sulfide species, ZnS precipitates more slowly (Mulkidjanian 2009). On the other hand, Zn can be stripped and remobilized from buried chimney fragments, and concentrated at the

Table 1 Specific surface area and average crystallite size of different ZnS samples. The crystallite sizes were estimated from the line broadening of the XRD peaks using the Scherrer's equation

| Catalyst	Specific area (m^2/g)	Crystallite size (nm)
ZnS-1	138.4	2.6
ZnS-2	154.0	5.5
ZnS-3	147.5	10.5
ZnS-4	167.2	12.9
ZnS-5	106.8	14.3

Fig. 4 Yields of (**a**) glutamate (□, ■) and valine (▲, △) and (**b**) α-ketoglutarate (□, ■) and α-ketoisovalerate (▲, △) in the amination and deamination experiments, respectively. The experimental conditions were similar to that in Fig. 1
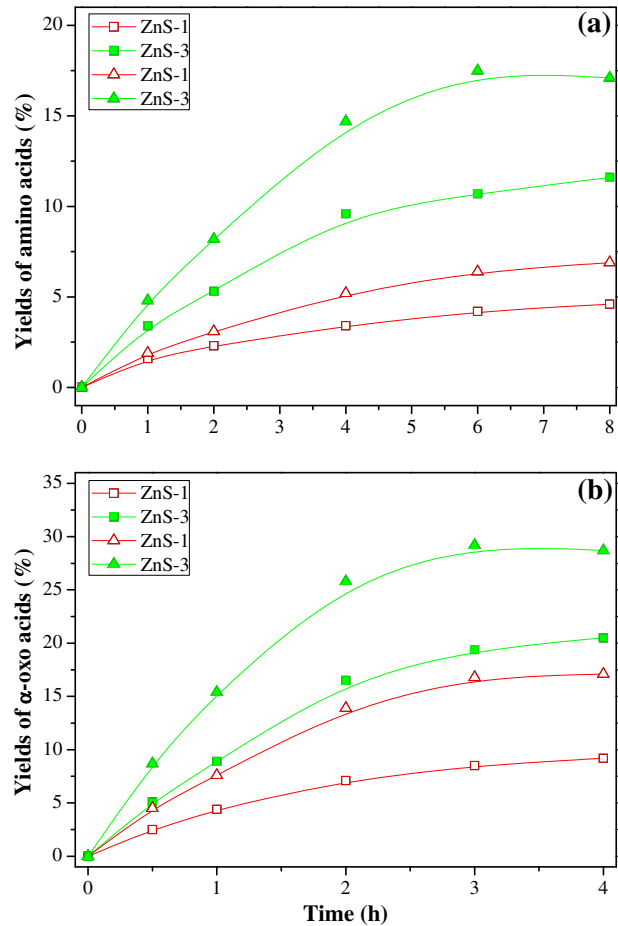
seawater interface (Edmond et al. 1995). Therefore, ZnS is a prevalent constitute at the periphery of hydrothermal deposits. If the hydrothermal vents on early Earth were located at a shallow depth no more than 100 m which consisted of the "photic zone" of primitive ocean, sunlight could penetrate the waters of early Earth to trigger prebiotic synthesis on ZnS surfaces (Guzman and Martin 2009). ZnS could absorb solar light to catalyze CO_2 fixation (Eggins et al. 1993) and molecular chain extension (Zhang and Martin 2006; Guzman and Martin 2009). Through such cascading reactions, a series of α-oxo acids such as glyoxylate, pyruvate, and α-ketoglutarate were produced. These acids are key intermediates or precursors of the reductive tricarboxylic acid (rCTA) cycle (Wang et al. 2012). Thus the mineral sphalerite (ZnS) may have played an important role in the prebiotic synthesis of biomolecules and the crucial evolutionary nascence of ancient metabolic pathways.

To understand the chemical emergence of life, it is of key importance to know what biomolecules and their metabolic pathways are used and shared by extant organisms. In the meantime, to uncover how life originated on early Earth, it is essential to know what organic compounds and their reaction channels were likely to have been available before the emergence of archaic enzymes. As is well known, amino acids are key building blocks for all terrestrial life forms. They serve as precursors for the biosynthesis of lipids,

carbohydrates, and nucleic acids. Following the fate of their carbon atoms, they can be traced to all important metabolic intermediates because of their close interaction with many biochemical processes such as the rTCA cycle. In view of the multitude of reversible pathways in the whole metabolic system, the homeostasis of amino acid molecules are very essential for the survival of life. In living organisms, reversible amination of α-keto acids exists in the biosynthesis of all proteinic amino acids. Glutamate dehydrogenase and transaminase participate in the regulation of the equilibria among amino acids and α-oxo acids. In various bacteria, a similar function is performed by a family of amino acid dehydrogenase (AADH) (Nitta et al. 1974; Oikawa et al. 2001). The latter catalyzes the reversible transformation between almost all proteinic amino acids and their corresponding oxo acids (Mohammadi et al. 2007),

$$\alpha-\text{oxo acid} + NH_3 + NAD(P)H^+ \xleftrightarrow{\text{AADH}} \text{amino acid} + H_2O + NAD(P)^+ \qquad (5)$$
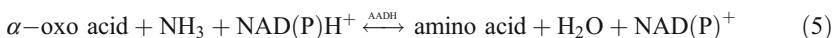
Especially, the substrates of some AADHs are nonspecific. One AADH can catalyze the reversible reaction of several amino acids (Nitta et al. 1974; Ohshima et al. 1990), even of non-protein amino acids (Krix et al. 1997). The AADH chemistry described above (Eq. 5) seems very like the reversible processes on ZnS surfaces (Eqs. 1–4). On the primitive sunlit and rocky planet, the prebiotic synthesis began with carbon and nitrogen fixation in the shallow-water hydrothermal vent systems (Zhang and Martin 2006; Guzman and Martin 2009). A series of α-oxo acids was formed therein. Starting with these acids and ammonia, photo-illuminated ZnS triggered the primordial synthesis of amino acids,

$$RCOCOO^- + NH_3 + 2H^+ \xleftrightarrow{\text{ZnS,hv}} RCH(NH_2)COO^- + H_2O \qquad (6)$$

In the backward direction, the amino acid products could be oxidized back to oxo acids, maintaining the prebiotic redox homeostasis of amino acid metabolism. Accordingly, we would expect that the enzyme-assisted reversible amination of α-keto acids might evolve from a ZnS-photo-promoted geochemical reaction pathway.

Conclusions

In this paper, we suggest a prototypical model for the origin of prebiotic metabolism, as well as demonstrating a simple photocatalytic reaction pathway. In the Hadean Eon, the world was trackless for metabolism. But later on, many a path was worn by geochemical processes on mineral surfaces during the initial phase of the formation of prebiotic metabolic systems. Thereafter in the evolutionary context, along with the polymerization of amino acids on the rocks (Orgel 1998; Wächtershäuser 2007) and the emergence of archaic proteins and enzymes, the enzyme-like chemistry of the minerals was replaced by primordial enzymatic networks. This is a process of metabolic takeover. The organic polymers found a way to dispense with the primitive surface metabolism. They arranged for the existence of better catalysts of their precursors than the minerals could manage to build. In the submarine hydrothermal niche market, since the reaction channels were well arranged by the minerals, the species of available metabolic substrates and intermediates were limited. By arrangement rather than by chance, the last universal common ancestor spontaneously tracked the footprints of the minerals and then faithfully inherited the geochemical metabolic pathways, which eventually evolved into the metabolism as we know it today.

References

Baross JA, Hoffman SE (1985) Submarine hydrothermal vents and associated gradient environments as sites for the origin and evolution of life. Orig Life 15:327–345

Boiteau L, Pascal R (2011) Energy sources, self-organization, and the origin of life. Orig Life Evol Biosph 41:23–33

Bonifačić M, Štefanić I, Hug GL, Armstrong DA, Asmus K (1998) Glycine decarboxylation: the free radical mechanism. J Am Chem Soc 120:9930–9940

Cairns-Smith AG (2008) Chemistry and the missing era of evolution. Chem Eur J 14:3830–3839

Corliss JB, Dymond J, Gordon LI, Edmond JM, von Herzon RP, Ballard RD, Green K, Williams D, Bainbridge A, Crane K, van Andel TH (1979) Submarine thermal springs on the Galápagos Rift. Science 203:1073–1083

Edmond JM, Campbell AC, Palmer MR, Klinkhammer GP, German CR, Edmonds HN, Elderfield H, Thompson G, Rona P (1995) Time series studies of vent fluids from the TAG and MARK sites (1986, 1990) Mid-Atlantic Ridge: a new solution chemistry model and a mechanism for Cu/Zn zonation in massive sulphide orebodies. Geol Soc Spec Publ 87:77–86

Eggins BR, Robertson PKJ, Stewart JH, Woods E (1993) Photoreduction of carbon dioxide on zinc sulfide to give four-carbon and two-carbon acids. Chem Commun 349–350

Fry I (2011) The role of natural selection in the origin of life. Orig Life Evol Biosph 41:3–16

Guzman MI, Martin ST (2009) Prebiotic metabolism: production by mineral photoelectrochemistry of alpha-ketocarboxylic acids in the reductive tricarboxylic acid cycle. Astrobiology 9:833–842

Hartman H (1975) Speculations on the origin and evolution of metabolism. J Mol Evol 4:359–370

Hazen RM (2001) Life's rocky start. Sci Am 284:76–85

Holm NG (1992) Why are hydrothermal systems proposed as plausible environments for the origin of life. Orig Life Evol Biosph 22:5–14

Huber C, Wächtershäuser G (2003) Primordial reductive amination revisited. Tetrahed Lett 44:1695–1697

Krix G, Bommarius AS, Drauz K, Kottenhahn M, Schwarm M, Kula MR (1997) Enzymatic reduction of α-keto acids leading to L-amino acis, D- or L-hydroxy acids. J Biotechnol 53:29–39

Martin W, Baross J, Kelley D, Russell MJ (2008) Hydrothermal vents and the origin of life. Nat Rev Microbiol 6:805–814

Mohammadi HS, Omidinia W, Lotfi AS, Saghiri R (2007) Preliminary report of NAD$^+$-dependent amino acid dehydrogenase producing bacteria isolated from soil. Iran Biomed J 11:131–135

Morowitz H, Smith E (2007) Energy flow and the organization of life. Complexity 13:51–59

Mulkidjanian AY (2009) On the origin of life in the Zinc world: I. Photosynthesizing, porous edifices built of hydrothermally precipitated zinc sulfide as cradles of life on Earth. Biol Direct 4:26

Nitta Y, Yasuda Y, Tochikubo K, Hachisuka Y (1974) L-amino acid dehydrogenases in *Bacillus subtilis* spores. J Bacteriol 117:588–592

Ohshima T, Sakane M, Yamazaki T, Soda K (1990) Thermostable alanine dehydrogenase from thermophilic *Bacillus sphaericus* DSM 462. Purification, characterization and kinetic mechanism. Eur J Biochem 191:715–720

Ohtani B, Kawaguchi J, Kozawa M, Nishimoto S, Inui T, Izawa K (1995) Photocatalytic racemization of amino acids in aqueous polycrystalline cadmium(II) sulfide dispersions. J Chem Soc Faraday Trans 91:1103–1109

Oikawa T, Yamanaka K, Kazuoka T, Kanzawa N, Soda K (2001) Psychrophilic valine dehydrogenase of the antarctic psychrophile, *Cytophaga* sp. KUC-1: purification, molecular characterization and expression. Eur J Biochem 268:4375–4383

Orgel LE (1998) Polymerization on the rocks: theoretical introduction. Orig Life Evol Biosph 28:227–234

Russell MJ, Hall AJ (1997) The emergence of life from iron monosulphide bubbles at a submarine hydrothermal redox and pH front. J Geol Soc 154:377–402

Russell MJ, Martin W (2004) The rocky roots of the acetyl-CoA pathway. Trends Biochem Sci 29:358–363

Simoncini E, Russell MJ, Kleidon A (2011) Modeling free energy availability from Hadean hydrothermal systems to the first metabolism. Orig Life Evol Biosph 41:529–532

Wächtershäuser G (1988) Before enzymes and templates: theory of surface metabolism. Microbiol Rev 52:452–484

Wächtershäuser G (2007) On the chemistry and evolution of the pioneer organism. Chem Biodiver 4:584–602

Wang W, Yang B, Qu Y, Liu X, Su W (2011) FeS/S/FeS$_2$ redox system and its oxidoreductase-like chemistry in the Iron-sulfur World. Astrobiology 11:471–476

Wang W, Li Q, Liu X, Yang Y, Su W (2012) Photocatalytic reversible amination of α-keto acids on a ZnS surface: implications for the prebiotic metabolism. Chem Commun 48:2146–2148

Xu Y, Schoonen MAAA (2000) The absolute energy positions of conduction and valence bands of selected semiconducting minerals. Am Mineral 85:543–556

Zhang XV, Martin ST (2006) Driving parts of Krebs cycle in reverse through mineral photochemistry. J Am Chem Soc 128:16032–16033